



HAL
open science

Colocalization of Wnt/ β -Catenin and ACTH Signaling Pathways and Paracrine Regulation in Aldosterone-producing Adenoma

Kelly de Sousa, Alaa Abdellatif, Isabelle Giscos-Douriez, Tchao Meatchi, Laurence Amar, Fabio Fernandes-Rosa, Sheerazed Boulkroun, Maria-Christina Zennaro

► **To cite this version:**

Kelly de Sousa, Alaa Abdellatif, Isabelle Giscos-Douriez, Tchao Meatchi, Laurence Amar, et al.. Colocalization of Wnt/ β -Catenin and ACTH Signaling Pathways and Paracrine Regulation in Aldosterone-producing Adenoma. *Journal of Clinical Endocrinology and Metabolism*, 2022, 107 (2), pp.419-434. 10.1210/clinem/dgab707 . hal-03845880

HAL Id: hal-03845880

<https://hal.science/hal-03845880>

Submitted on 9 Nov 2022

HAL is a multi-disciplinary open access archive for the deposit and dissemination of scientific research documents, whether they are published or not. The documents may come from teaching and research institutions in France or abroad, or from public or private research centers.

L'archive ouverte pluridisciplinaire **HAL**, est destinée au dépôt et à la diffusion de documents scientifiques de niveau recherche, publiés ou non, émanant des établissements d'enseignement et de recherche français ou étrangers, des laboratoires publics ou privés.

Colocalization of Wnt/ β -catenin and ACTH signaling pathways and paracrine regulation in aldosterone producing adenoma

Kelly De Sousa^{1*}, Alaa B Abdellatif^{1*}, Isabelle Giscos-Douriez¹, Tchao Meatchi^{1,2}, Laurence Amar^{1,3}, Fabio L Fernandes-Rosa^{1§}, Sheerazed Boulkroun^{1§}, Maria-Christina Zennaro^{1,4#}

¹Université de Paris, PARCC, Inserm, Paris, France

²Assistance Publique-Hôpitaux de Paris, Hôpital Européen Georges Pompidou, Service d'Anatomie Pathologique, Paris, France

³Assistance Publique-Hôpitaux de Paris, Hôpital Européen Georges Pompidou, Unité Hypertension artérielle, Paris, France

⁴Assistance Publique-Hôpitaux de Paris, Hôpital Européen Georges Pompidou, Service de Génétique, Paris, France

*.§These authors contributed equally to this work

#Corresponding author

Address correspondence to:

Maria-Christina Zennaro, MD, PhD

Inserm, U970

Paris Cardiovascular Research Center – PARCC

56, rue Leblanc,

75015 Paris – France

Tel : +33 (0)1 53 98 80 42

Fax : + 33 (0)1 53 98 79 52

e-mail : maria-christina.zennaro@inserm.fr

Running Title: Signaling pathways in APA

Abbreviations: PA, primary aldosteronism; APA, aldosterone producing adenoma;

Word count – Abstract: 248

Word count – manuscript: 4175

Number of figures: 11

Number of tables: 1

Declaration of interest

The authors have nothing to disclose

1 **Abstract**

2 **Context.** Aldosterone-producing adenomas (APA) are a common cause of primary
3 aldosteronism. Despite the discovery of somatic mutations in APA and characterization of
4 multiple factors regulating adrenal differentiation and function, the sequence of events leading
5 to APA formation remains to be determined.

6 **Objective.** We investigated the role of Wnt/ β -catenin and ACTH signaling, as well as elements
7 of paracrine regulation of aldosterone biosynthesis in adrenals with APA and their relationship
8 to intratumoral heterogeneity and mutational status.

9 **Design.** We analyzed expression of CYP11B2, CYP17A1, β -catenin, MC2R, pCREB,
10 Tryptase, S100, CD34 by multiplex immunofluorescence and IHC guided RT-qPCR.

11 **Setting.** 11 adrenals with APA and one with micronodular hyperplasia from patients with PA
12 were analysed.

13 **Main Outcome Measure(s).** Localization of CYP11B2, CYP17A1, β -catenin, MC2R, pCREB,
14 Tryptase, S100, CD34 in APA and aldosterone producing cell clusters (APCC).

15 **Results.** Immunofluorescence revealed abundant mast cells and a dense vascular network in
16 APA, independent of mutational status. Within APA, mast cells were localized in areas
17 expressing CYP11B2 and were rarely co-localized with nerve fibers, suggesting that their
18 degranulation is not controlled by innervation. In these same areas, β -catenin was activated,
19 suggesting a zona glomerulosa cell identity. In heterogeneous APA with *KCNJ5* mutations,
20 *MC2R* and *VEGFA* expression was higher in areas expressing CYP11B2. A similar pattern was
21 observed in APCC, with high expression of CYP11B2, activated β -catenin, and numerous mast
22 cells.

23 **Conclusions.** Our results suggest that aldosterone producing structures in adrenals with APA
24 share common molecular characteristics and cellular environment, despite different mutation
25 status, suggesting common developmental mechanisms.

26

27 **Key words:** Aldosterone, Mineralocorticoids, Endocrine Hypertension, Primary
28 Aldosteronism, Aldosterone producing adenoma, Adrenal Cortex, signalling pathway,
29 paracrine regulation, mast cells, vessels

30 **Introduction:**

31 Aldosterone producing adenomas (APA) and bilateral adrenal hyperplasia are the main causes
32 of primary aldosteronism (PA) (1). PA is the most frequent form of secondary arterial
33 hypertension with a prevalence of 5% of hypertensive patients in primary care and up to 10%
34 of those seen in reference centers (2-4). Hypertension, increased aldosterone levels with
35 suppressed plasma renin, and in many cases hypokalemia are the main characteristics of the
36 disease. Patients with PA are at excess risk for cardiovascular events when compared to patients
37 with primary hypertension (5,6).

38 Different somatic mutations in APA and germline mutations in familial PA were discovered
39 using whole exome sequencing approaches. These mutations affect genes coding for ion
40 channels (*KCNJ5*, *CACNA1D*, *CACNA1H*, *CLCN2*) or ATPases (*ATP1A1*, *ATP2B3*) (7). They
41 lead to autonomous aldosterone production by increasing the expression of *CYP11B2*, coding
42 for aldosterone synthase. The prevalence of somatic mutations is estimated between 88 and
43 96% by immunohistochemistry-guided next-generation sequencing (NGS) (8-12). Other
44 autonomous aldosterone producing lesions were described in normal adrenals as well as in
45 peritumoral tissue in adrenals with APA. Indeed, somatic mutations in *CACNA1D*, *ATP1A1* and
46 *KCNJ5* have been described in APCC (aldosterone producing cell clusters, also called
47 aldosterone producing nodules (13)) and pAATL (possible APCC to APA translational lesions)
48 (10,14,15). The recurrence of somatic mutations in APA driver genes and the metabolic profile
49 of APCC suggested that they may induce APA development (14).

50 In addition to genes coding for ion channels and pumps, mutations in genes related to adrenal
51 development, maintenance of the zona glomerulosa (ZG) and steroidogenesis were also
52 described in APA. Particularly, somatic mutations in *CTNNB1* coding for β -catenin are found
53 in 2% to 5% of cases (16,17), possibly causing a proliferative advantage in adrenal cells and an

54 abnormal activation of WNT signaling pathway. More recently, somatic mutations in
55 *GNAQ/GNA11* were identified in APA carrying somatic *CTNNB1* mutations in patients
56 presenting with PA in puberty, pregnancy or menopause (18). Somatic mutations in *PRKACA*
57 (catalytic subunit of protein kinase A) are rare findings in APAs and their direct involvement
58 in APA development is still unclear (19). The Wnt/ β -catenin pathway plays a role in the identity
59 and function of ZG cells, whereas the ACTH/cAMP pathway is involved in the differentiation
60 of ZG cells into zona fasciculata (ZF) cells by inhibiting the Wnt/ β -catenin pathway (20) as
61 well as in regulating glucocorticoid biosynthesis. We have previously reported that in APA the
62 Wnt/ β -catenin pathway was activated mainly in areas expressing aldosterone synthase (10),
63 supporting its role in maintaining ZG cell identity and function (21). The observed intratumoral
64 heterogeneity in APA suggested that the interplay between ACTH/cAMP and Wnt/ β -catenin
65 pathways may be involved in the transdifferentiation of ZG cells into ZF cells within the APA.

66 Aldosterone production is regulated by the renin-angiotensin system, potassium concentrations
67 and, to a lesser extent, by the adrenocorticotrophic hormone (ACTH) (22). When binding to its
68 receptor (melanocortin type 2 receptor-MC2R), ACTH activates adenylate cyclase (AC) and
69 protein kinase A (PKA), which phosphorylates CREB (cAMP response element binding
70 protein) resulting in increased StAR (steroidogenic acute regulatory protein) expression (23).
71 In addition, paracrine regulation of aldosterone production is mediated by factors released by
72 components of the APA microenvironment, i.e. chromaffin cells, endothelial cells, nerve fibers
73 and immune cells (24-27). Serotonin (5-HT) released by perivascular mast cells is known to
74 induce aldosterone production. Different signals may stimulate mast cell degranulation such as
75 neurotransmitters, neuropeptides and hormones (28). However, the control of mast cell
76 degranulation in the adrenal gland is not well clarified (24,29). A peculiar feature of the adrenal
77 gland is also the very high expression of VEGF, even in adulthood, despite the absence of active
78 angiogenesis (30,31). ACTH controls the coordinated development of vessels and endocrine

79 cells. In this context, the role of *VEGFA*, whose expression is controlled by ACTH, is to
80 maintain a high density of stable fenestrated microvessels (30,31). The combined secretion of
81 angiogenic factors by endocrine cells and trophic factors by endothelial cells allows the
82 maintenance of a "symbiosis" between these cellular compartments.

83 The aim of this study was to investigate the relationship between different signaling pathways
84 and components of the microenvironment in adrenals with APA to better understand the
85 mechanisms driving the development of aldosterone producing structures and intratumoral
86 heterogeneity. We performed detailed morphological investigations of 11 adrenals with APA
87 and one with micronodular hyperplasia using multiplex immunofluorescence multispectral
88 image analysis. In addition, CYP11B2 IHC guided RT-qPCR was performed on RNA extracted
89 from formalin-fixed paraffin-embedded (FFPE) tissues in 7 adrenals. Results were correlated
90 with the APA mutation status.

91

92 **Materials and methods:**

93 *Patients*

94 Patients included in this study underwent adrenalectomy between 2013 and 2016 at the Hôpital
95 Européen Georges Pompidou and were recruited within the COMETE-HEGP protocol
96 (authorization CPP 2012-A00508-35) and are described in (10). Screening and subtype
97 identification of PA were performed according to institutional and Endocrine Society guidelines
98 (32-34), 16 adrenals from patients with APA and two adrenal blocs from one patient with
99 multinodular hyperplasia were investigated for a total of 18 samples from 17 patients (Table 1).
100 All patients gave written informed consent for genetic and clinical investigation. Procedures
101 were in accordance with institutional guidelines. APA mutational status has been described in
102 (10).

103 *Multiplex immunofluorescence*

104 Multiplex immunofluorescence staining was performed with the Opal 7-color Manual IHC Kit
105 (PerkinElmer) in two separate sets of experiments. Sections were deparaffinised in xylene and
106 rehydrated through graded ethanol before washing with distilled water and TBST (0.1 M Tris-
107 HCl, pH 7.5, 0.15 M NaCl, 0.05 % Tween 20). Sections were re-fixed by 20 min incubation in
108 4% paraformaldehyde followed by a distilled water wash. The slides were incubated in AR6
109 buffer (1/10; PerkinElmer) and subjected to microwave treatment for 15 minutes at 20% power
110 for antigen unmasking. Nonspecific staining was blocked with blocking solution (PerkinElmer)
111 for 10 minutes. Given the complexity of the setup of multiplex immunofluorescence either
112 CYP11B1 or CYP17A1 were used to identify ZF cells.

113 For a first multiplex immunofluorescence, the slides were incubated with a mouse monoclonal
114 antibody against aldosterone-synthase (1/100, hCYP11B2, clone 41-13C, kindly provided by
115 Dr C Gomez-Sanchez, RRID: [AB_2650562](https://europepmc.org/abstract/proc/abn/AB_2650562)), rabbit polyclonal antibody against 17 α -

116 hydroxylase (1/1000, LSBio #LS-B14227, RRID: [AB_2857939](#)), mouse monoclonal antibody
117 against β -catenin (1/400 ; BD Biosciences #610153, RRID: [AB_397554](#)), rabbit polyclonal
118 antibody against MC2R (1/200, Abgent #AP5540b, RRID: [AB_10820209](#)), and a rabbit
119 monoclonal antibody against pCREB (Ser133) (1/500, Cell signaling technology #9198, RRID:
120 [AB_2561044](#)). For a second multiplex immunofluorescence, the slides were incubated with a
121 mouse monoclonal antibody against mast cell tryptase (1/10000, BIO-RAD #MCA1438, RRID:
122 [AB_2206190](#)), rabbit monoclonal antibody against S100 protein (1/2, Agilent #GA50461-2,
123 RRID: [AB_2811056](#)), antibody against 11 β -hydroxylase (1/100, hCYP11B1-80-2-2, kindly
124 provided by Dr C Gomez-Sanchez, RRID: [AB_2650563](#)), and a mouse monoclonal antibody
125 against CD34 (1/5000, ThermoFisher #MA1-10202, RRID: [AB_11156010](#)) during 1h at room
126 temperature. Sections were washed and incubated with secondary antibody working solution
127 (PerkinElmer) during 10 minutes; for CYP11B1 the slides were incubated with an anti-rat
128 secondary antibody (1/400, ImmPRESS Anti-Rat IgG, Vector Laboratories #MP-7404, RRID:
129 [AB_2336531](#)) during 1h at room temperature. Then, slides were incubated for 10 minutes in
130 TSA plus solution (included in the Opal 7-color manual IHC kit to detect antibody staining),
131 prepared according to the manufacturer's instructions: Opal 570 (1/100), Opal 650 (1/100 -
132 1/200 for S100), Opal 690 (1/50), Opal 540 (1/50 - 1/100 for CYP11B1), Opal 520 (1/50), Opal
133 620 (1/200). Microwave treatment was performed to remove primary and secondary antibodies
134 while retaining an intact fluorescent signal. This process was repeated until all targets of interest
135 were detected, using the respective Opal fluorophore for each one. The slides were
136 counterstained with DAPI (PerkinElmer) for 5 minutes.

137 ***Immunohistochemistry***

138 Sections were deparaffinised in xylene and rehydrated through graded ethanol. For antigen
139 unmasking, the slides were incubated 30 min at 98°C in Trilogy solution (1/20) (Sigma-Aldrich;
140 St Louis, MO USA) for aldosterone-synthase (CYP11B2) and 11 β -hydroxylase (CYP11B1)

141 immunohistochemistry, or in a citrate solution (0.935%, Vector Laboratories; Burlingame,
142 USA) for immunostaining against CD34, mast cell tryptase, pCREB, MC2R and β -catenin. No
143 antigen unmasking was performed for S100 immunostaining. Endogenous peroxidases were
144 inhibited by incubation in 3% hydrogen peroxide (Sigma-Aldrich) for 10 min. Nonspecific
145 staining was blocked with filtered Tris 0.1 M pH 7.4, 10% normal goat serum, 10% bovine
146 serum albumin, and 0.1% SDS for 90 min (for 11 β -hydroxylase staining); filtered Tris 0.1 M
147 pH 7.4, 10% horse serum and 0.5% SDS for 60 min (for aldosterone-synthase staining) or with
148 PBS 1x and 10% normal goat serum for 30 mins (for CD34, mast cell tryptase, S100, β -catenin,
149 MC2R, and pCREB stainings). The slides were incubated overnight at 4°C (aldosterone-
150 synthase, 11 β -hydroxylase, and pCREB stainings) or during 1h at room temperature (β -catenin
151 MC2R, mast cell tryptase, S100 protein and CD34 stainings), using the same antibodies and
152 same dilutions described for multiplex immunofluorescence experiments. Sections were
153 washed, incubated 30 min with affinity purified horse anti mouse secondary antibody for
154 aldosterone-synthase, β -catenin, CD34 and mast cell tryptase stainings (1/400, Vector
155 Laboratories #BP-2000, RRID: [AB 2687893](#)), rabbit anti rat antibody for 11 β -hydroxylase
156 antibody (1/400, Vector Laboratories #BA-4001, RRID: [AB 10015300](#)), or an anti-rabbit
157 secondary antibody for MC2R, S100 and pCREB stainings (1/400, Vector Laboratories #BA-
158 1000, RRID: [AB 2313606](#)). Slides were washed and incubated with an avidin-biotin-
159 peroxydase complex (Vectastain ABC Elite; Vector Laboratories) for 30 min. The slides were
160 developed using diaminobenzidin (Vector Laboratories; Burlingame, USA) and counterstained
161 with hematoxilin (Sigma-Aldrich; St Louis, MO USA).

162 *Analysis and quantification of histological features*

163 Multiplex immunofluorescence and immunohistochemistry images were acquired using a
164 Vectra® automated imaging system and automatically quantified with the InForm® image
165 analysis package (both Perkin Elmer; Waltham, USA). Each monoplex biomarker was used to

166 generate the spectral library required for multispectral analysis. Tryptase positive cells and S100
167 positive fibers were counted as objects, and CD34 positive vessels as area based on their
168 staining in CYP11B2 expressing and non expressing areas. The quantification of these markers
169 was automatically performed with inForm. Areas in 11 APA were selected to allow the
170 determination of colocalization of aldosterone-synthase (CYP11B2), 17 α -hydroxylase
171 (CYP17A1), MC2R, pCREB and cytoplasmic and nuclear staining for β -catenin, which was
172 automatically quantified using InForm® (Perkin Elmer; Waltham, USA).
173 The distance between mast cells and nerve fibers was measured using the Icy software
174 (<http://icy.bioimageanalysis.org/>).

175 ***RNA extraction and RT-qPCR***

176 RNA was co-extracted with DNA from formalin-fixed paraffin-embedded (FFPE) sections
177 using AllPrep DNA/RNA FFPE kit (Qiagen). Before extraction, APA and aldosterone
178 producing cell clusters (APCC) were identified by CYP11B2 immunohistochemistry (IHC) as
179 described in (10). Based on the CYP11B2 IHC, the areas of interest were delineated and isolated
180 for DNA and RNA extraction by scraping unstained FFPE sections guided by the CYP11B2
181 IHC slide using a scalpel under a Wild Heerbrugg microscope.

182 250 ng of total RNA were retrotranscribed (iScript reverse transcriptase, Biorad, Hercules, CA).
183 Primers used for amplification of *MC2R* (qHsaCEP0054989) and *MRAP* (qHsaCID0022591)
184 were purchased from BioRad. The sequence of primers used for *MRAP2*, *VEGFA*, *18S*, and
185 *GAPDH* can be provided upon request. Quantitative PCR was performed using SYBRgreen
186 (Sso advanced universal SyBr Green supermix, Biorad, Hercules, CA) on a C1000 touch
187 thermal cycler (Biorad CFX96 Real Time System), according to the manufacturer's instructions.
188 Controls without template were included to exclude primer dimer formation or PCR
189 contaminations. RT-qPCR products were analyzed in a post amplification fusion curve to
190 ensure that a single amplicon was obtained. Normalization for RNA quantity, and reverse

191 transcriptase efficiency was performed against two reference genes (geometric mean of the
192 expression of Ribosomal *18S* and *GAPDH* RNA). Quantification was performed using the
193 standard curve method. Standard curves were generated using serial dilutions from a cDNA
194 pool of all samples of each experiment, yielding a correlation coefficient of at least 0.98 in all
195 experiments.

196 *Statistical Analyses*

197 Quantitative variables are reported as mean +/- SEM. Comparisons between groups were done
198 with unpaired t-test when Gaussian distribution or the Mann-Whitney test when no Gaussian
199 distribution. A p value < 0.05 was considered significant for comparisons between 2 groups.

200

201

202 **Results**

203 **Elements of paracrine regulation of aldosterone biosynthesis in APA**

204 11 adrenals with APA were analysed by multiplex immunofluorescence to study the cellular
205 environment and markers of paracrine regulation: mast cells were labelled with tryptase, nerve
206 cells with S100, and vascular endothelial cells were labelled with CD34. In addition, the Wnt/ β -
207 catenin and ACTH/cAMP/PKA pathways involved in the maintenance and function of the
208 adrenal cortex were investigated (Figure 1). These APA carry somatic mutations previously
209 identified by Sanger sequencing and IHC-guided targeted NGS, including 2 *KCNJ5* mutations,
210 3 *CACNA1D* mutations, 3 *ATP1A1* mutations, and 3 *ATP2B3* mutations (Table 1).

211 Multiplex immunofluorescence revealed abundance of tryptase positive mast cells and a dense
212 vascular component in APA independently of the mutational status. Remarkably, in all APA
213 analysed, the majority of mast cells were found in areas expressing CYP11B2, in contrast to
214 areas not expressing CYP11B2 or areas expressing CYP11B1 ($p < 0.0001$) (Figure 2A-B). There
215 was no difference of vascular surface between CYP11B2 expressing and non-expressing areas
216 ($p = 0.1214$) (Figure 2C). APA also contained nerve fibers whose localisation was independent
217 of the expression of CYP11B2 ($p = 0.6614$) (Figure 2D). Remarkably, colocalization of mast
218 cells and nerve fibers, which would suggest innervation of mast cells, was rarely observed
219 (Figure 3A). Indeed, measurement of the distance between mast cells and nerve fibers in the 11
220 APA included in our study showed a mean distance between immune cells and nerve fibers of
221 80.27 μm , with important intratumoral heterogeneity (Figure 3B). Multiplex
222 immunofluorescence on selected areas revealed cellular co-expression of CYP11B2 with
223 activated i.e. nuclear and/or cytoplasmic staining of β -catenin in the majority of cells, in contrast
224 to areas expressing CYP17A1, independently of the mutational status of APA, as previously
225 described (10) (Figure 1).

226 Finally, mast cells were found both within the APA and in the adjacent adrenal cortex, often in
227 close proximity to vascular cells (Figure 4).

228

229 **Expression of components of ACTH signaling and vascularization**

230 Expression of MC2R was more frequently observed in CYP11B2 positive areas in comparison
231 to areas expressing CYP17A1. Among cells expressing CYP11B2, 68% coexpress MC2R; in
232 contrast, only 15% of CYP17A1 positive cells express also MC2R and this pattern is
233 independent of the mutation status (Figure 5A-B). Expression of pCREB in APA was observed
234 in \approx 11% of cells and mainly observed in APA with *CACNA1D* mutations. pCREB does not
235 appear to be co-localized with CYP11B2 nor CYP17A1 in any of the mutational groups (Figure
236 5C-D). Co-expression of pCREB in cells expressing MC2R was also low (Figure 5E)
237 suggesting that MC2R expression is not correlated to PKA signaling in those cells.

238 For a better understanding of the control of the ACTH/cAMP signaling pathway in APA and
239 its interaction with the vascular component, the expression of *MC2R*, *MRAP*, *MRAP2* and
240 *VEGFA* was investigated by RT-qPCR in five APA included in the multiplex
241 immunofluorescence study. Three APA carried a *CACNA1D* mutation, one carried an *ATP2B3*
242 mutation and in one APA no mutation had been identified; in addition, a nodule not expressing
243 CYP11B2 and not carrying somatic mutations in any of the APA driver genes was included
244 (Table 1, Figure 6A-B). In addition, different areas expressing or not CYP11B2 from two APA
245 carrying *KCNJ5* mutations were also analysed by RT-qPCR (Figure 7A).

246 *MC2R* mRNA was expressed in three out of four APA included in our study, although at
247 different levels (Figure 6C). Interestingly, in one adrenal gland presenting a small APA and a
248 large nodule not expressing CYP11B2, *MC2R* was expressed only in the APA, but not in the
249 CYP11B2 negative nodule (Figure 6C). MRAP and MRAP2 are accessory proteins for MC2R

250 signaling (35). *MRAP* expression was observed in APA from patients 25 (non-mutated), 42
251 (*CACNA1D* mutated) and 56 (*ATP2B3* mutated) (Figure 6D), but not in APA from patients 10
252 and 34 (*CACNA1D* mutated); *MRAP2* was not expressed in any of the samples (data not shown).
253 Within heterogeneous APA carrying *KCNJ5* mutations (Figure 7A), the expression of the
254 *MC2R* gene was higher in areas expressing CYP11B2 in comparison to areas not expressing
255 CYP11B2 (Figure 7B). *MRAP* was expressed heterogeneously in APA but independently of
256 CYP11B2 expression (Figure 7C), while again *MRAP2* expression was not found (data not
257 shown).

258 The expression of *VEGFA* was found in all APA as well as in the CYP11B2 negative nodule of
259 patient 56, independently of the APA mutation status (Figure 6E). Within heterogeneous APA,
260 expression of *VEGFA* was higher in areas expressing CYP11B2 in comparison to areas not
261 expressing CYP11B2, and grossly followed the pattern of *MC2R* expression in the majority of
262 zones investigated (Figure 7D).

263

264 **ACTH and β -catenin signaling pathways and paracrine regulation in other aldosterone** 265 **producing lesions from adrenals with APA**

266 Within our adrenal samples, several APCC and secondary nodules not expressing CYP11B2
267 were present, including multiple APCC in one adrenal with micronodular hyperplasia. The
268 mutational status of 13 APCC from three adrenals carrying an APA, and four APCC and one
269 pAATL from one adrenal with micronodular hyperplasia had previously been assessed by
270 CYP11B2 immunohistochemistry-guided NGS (10). Three APCC carried *KCNJ5* mutations,
271 seven carried *CACNA1D* mutations and in seven APCC no mutations were identified (Table 1).
272 Remarkably, all APCC in adrenals with APA or with micronodular hyperplasia showed
273 cytoplasmic and/or nuclear β -catenin coexpressed with CYP11B2, independently of the

274 mutational status; nuclear pCREB expression was also observed, indicating an activation of
275 both signaling pathways in APCC (Figure 8). For technical reasons, in these structures
276 acquisition of MC2R labeling on Opal was not possible, thus MC2R expression in the same
277 APCC was investigated by IHC. MC2R was strongly expressed at the membrane and in the
278 cytoplasm of cells composing the APCC (Figure 9). Nuclear pCREB was also strongly
279 expressed in the APCC, as well as in the ZG, similar to activated β -catenin (Figure 8).
280 Remarkably, accumulation of mast cells was observed around APCC with a reorganization of
281 the vascular network, where the centripetal capillaries follow the CYP11B2 positive cells
282 (Figure 8); in some cases, mast cells were observed in close proximity to vascular cells (Figure
283 4). Nerve fibers labeled by S100 were hardly detected in APCC.

284 Remarkably, in the pAATL the outer part expresses CYP11B2 and the inner part is CYP17A1
285 positive (Figure 10). Activated β -catenin, a reduced vascular network, nuclear pCREB
286 expression and an abundant number of mast cells were observed in the external part of the
287 structure coexpressed with CYP11B2 (Figure 10). In contrast, the inner part of the pAATL did
288 not express activated β -catenin and pCREB, showed a more organised vascular network and
289 less mast cells. MC2R expression was homogeneous in the pAATL (Figure 10). This
290 differential pattern was observed, although the inner and outer part of the pAATL carry the
291 same *CACNA1D* mutation (Table 1).

292 A secondary nodule non-expressing CYP11B2 from patient 56 was also analysed. This nodule,
293 which does not carry a somatic mutation (Table 1), expresses CYP17A1, shows nuclear
294 expression of pCREB and heterogeneous expression of activated β -catenin but no expression
295 of MC2R (Figure 11).

296

297 **Discussion**

298 The Wnt/ β -catenin, ACTH/cAMP/PKA signaling pathways and paracrine pathways play an
299 important role in steroidogenesis and adrenal development (36), but their role in the
300 development of APA and other aldosterone producing structures in the context of somatic
301 mutations as well as their interactions remain unclear. Although previous studies have
302 investigated individual components of this pathways independently, here we applied multiplex
303 immunofluorescence and multispectral image analysis to investigate proteins involved in
304 aldosterone (CYP11B2) and cortisol (CYP11B1/CYP17A1) biosynthesis, in addition to
305 markers of Wnt/ β -catenin (β -catenin) and ACTH/cAMP/PKA (MC2R, pCREB) signaling, as
306 well as paracrine pathways of the tumor microenvironment (Tryptase, S100) and
307 vascularisation (CD34), in adrenals with APA and with micronodular hyperplasia. Our results
308 show a high abundance of mast cells and dense vascularisation in APA, which is independent
309 of the mutation status. Mast cells were mainly localized in zones expressing aldosterone
310 synthase within the tumour. In cells expressing aldosterone synthase, β -catenin is activated and
311 MC2R is highly expressed and found at the cell membrane; *VEGFA* expression was more
312 important in areas expressing CYP11B2 suggesting regulation by ACTH signaling. In APCC,
313 β -catenin is activated and co-expressed with aldosterone synthase; a high number of mast cells
314 are observed in these areas with a reorganisation of the blood vessels following the cellular
315 arrangement of steroidogenic cells. Strong nuclear pCREB expression was also observed in
316 these structures, together with MC2R expression.

317 Our results confirm that mast cells are abundant in APA (27). In addition, our study shows that
318 mast cells accumulate next to CYP11B2 positive cells in APA, supporting their specific
319 contribution to aldosterone biosynthesis. Indeed, several studies have demonstrated that mast
320 cells are able to stimulate aldosterone production through the secretion of serotonin and the
321 activation of intracellular calcium signaling (37-39). It is well known that the adrenal cortex is

322 richly innervated and contains vasoactive intestinal peptide, substance P and neuropeptide Y
323 peptidergic fibers, which may influence aldosterone synthesis through a paracrine regulation
324 (26). Although it has been shown that neuronal mechanisms are involved in mast cell activation
325 (24), supporting the possibility that the sympathetic system can influence the function of a
326 subgroup of APA, colocalization of mast cells and nerve fibers was rarely observed in APA in
327 our study, suggesting that mast cell degranulation is not primarily stimulated by nerve fibers.
328 These results are in accordance with previous work showing only occasionally contacts between
329 mast cells and nerve terms in APA tissues (24). However, although we have quantified between
330 50-100% of the surface of each APA, we cannot exclude that some interactions may have been
331 missed; also local concentrations of neurotransmitters may signal to mast cells at distance.

332 The Wnt/ β -catenin and ACTH/cAMP/PKA signaling pathways are both involved in cell
333 differentiation and function of the ZG and ZF. Although only \approx 5% of APA carry *CTNNB1*
334 mutations, β -catenin is activated in a majority of them (40). In certain cases, *CTNNB1* mutations
335 alone, arising in the ZG, may suffice to induce development of APA maintaining the ZG
336 phenotype of the tumor. In other cases, *CTNNB1* may contribute to tumor formation in APA
337 carrying other types of mutations, by promoting cell proliferation or nodule formation either as
338 a first hit due to somatic mutations or because of its activation due to mechanisms that need to
339 be identified. The two hit model is supported by the identification of somatic *GNAQ/GNA11*
340 mutations in *CTNNB1* mutated APA in patients with PA presenting at puberty, pregnancy or
341 menopause (18), as well as the occurrence of *KCNJ5* mutations in adrenals from patients with
342 FAP carrying germline APC mutations (41).

343 Previous studies have shown that the expression of MC2R is higher in APA compared to the
344 normal adrenal gland (42). Our results showed that MC2R was highly expressed in areas
345 expressing CYP11B2 in APA, a result which was confirmed by *MC2R* gene expression studies
346 of different regions of APA expressing or not CYP11B2. In contrast, expression of pCREB in

347 APA was low and did not show any particular colocalization with either CYP11B2, CYP17A1
348 or MC2R, suggesting that CREB phosphorylation is independent of MC2R activation in APA.
349 We further investigated the activity of the ACTH signaling pathway by studying two accessory
350 proteins MRAP and MRAP2 known to initiate or inhibit MC2R activation respectively (43).
351 While we did not observe any expression of *MRAP2*, the expression of *MRAP* was
352 heterogeneous and independent of CYP11B2 expression, both across APA and within
353 heterogeneous APA carrying *KCNJ5* mutations. Altogether, these results suggest that in APA,
354 ACTH may be involved in the regulation of aldosterone production by signaling through
355 MC2R/MRAP and activation of calcium rather than CREB signaling. Indeed, activation of
356 calcium signaling by ACTH has been previously shown, involving activation, through
357 phosphorylation via PKA, of voltage gated calcium channels (23,44,45).

358 APA are highly vascularized structures. Although we did not observe intratumoral
359 heterogeneity in vascularization by multiplex immunofluorescence, *VEGFA* expression was
360 more important in areas expressing CYP11B2 in contrast to areas not expressing CYP11B2.
361 The increase of *VEGFA* expression in these areas may be explained by the presence of
362 perivascular mast cells, which are involved in the maintenance of angiogenesis, as shown in
363 pancreatic islet tumors (46), or alternatively by the activation of the ACTH/cAMP pathway via
364 MC2R, as MC2R is highly expressed in these same regions. Indeed, in the adrenal gland, ACTH
365 stimulates the release of VEGF and the stabilisation of its mRNA (47). Furthermore, it has been
366 suggested that changes in the vascular supply of the adrenal cortex, due to phenomena of
367 atherosclerosis or high blood pressure, may influence the function of the adrenal cortex,
368 resulting in compensatory adrenal cortex hyperplasia and eventually nodulation (48).

369 Remarkably, investigation of APCC revealed similar patterns of expression as observed in
370 APA, although with some peculiar features. We observed abundant mast cells in APCC,
371 supporting a role for paracrine regulation of autonomous aldosterone production in these

372 structures. The localization of mast cells close to blood vessels and within CYP11B2 positive
373 areas suggest that they may influence mineralocorticoid production directly and/or via the blood
374 flow. Furthermore, all APCC in adrenals with APA or with micronodular hyperplasia showed
375 nuclear and/or cytoplasmic β -catenin coexpressed with CYP11B2, independently of the
376 mutational status. In contrast to APA, strong nuclear pCREB expression was also observed,
377 together with MC2R expression, suggesting ACTH signaling via PKA/pCREB in APCC.
378 MC2R was previously identified as a highly expressed gene in APCC (14). These results
379 indicate that in APCC both ACTH/cAMP as well as Wnt/ β -catenin signaling are activated,
380 suggesting that APCC may be intermediary structures in terms of cell lineage between the ZG
381 and the ZF. This hypothesis is supported by previous work showing characteristics of both ZG
382 and ZF within the same structures (49). The presence of mast cells in these structures may
383 contribute to the activation of PKA signaling pathway via serotonin/5HT4 signaling (50) and
384 be involved in the autonomous aldosterone production. The additional activity of the calcium
385 signaling pathway in regulating CYP11B2 expression and aldosterone production in APCC is
386 supported by the presence of somatic mutations in APA-driver genes that have been previously
387 shown to activate calcium signaling. These finding suggests that different signalling pathways
388 are involved in the development and maintenance of APCC.

389 Remarkably, in a nodule non expressing CYP11B2 from an adrenal with APA, mast cells were
390 present but localized to the areas not expressing CYP11B1 either. This is consistent with
391 previous studies showing that mast cell proliferation is observed in a deoxycorticosterone-
392 secreting tumor and APA but not in cortisol-secreting adenomas (51), suggesting that mast cells
393 may preferentially favour proliferation of glomerulosa cells (24) and mineralocorticoid
394 secretion.

395 In conclusion, our results show that aldosterone producing structures in adrenals with APA
396 share common molecular characteristics and cellular environment, despite different mutation

397 status, suggesting common developmental mechanisms. In particular, mast cells appear to be
398 closely associated with cells expressing aldosterone synthase, both in APA and APCC, and their
399 degranulation seems not to be regulated by innervation. In these same areas, activation of β -
400 catenin indicates a zona glomerulosa cell identity. Activation of PKA signalling was
401 heterogeneous in aldosterone producing structures, suggesting different signalling pathways
402 activated by ACTH and serotonin to drive aldosterone biosynthesis.

403

404

405 **Declaration of interest**

406 The authors have nothing to disclose

407 **Acknowledgments**

408 The authors wish to thank CE Gomez-Sanchez (University of Mississippi Medical Center,
409 Jackson, MS) for providing antibodies against CYP11B1 and CYP11B2.

410 **Funding**

411 This work was funded through institutional support from Inserm, the Agence Nationale de la
412 Recherche (ANR-15-CE14-0017-03), and the Fondation pour la Recherche Médicale
413 (DEQ20140329556).

414

415 **Data availability**

416 Some or all datasets generated during and/or analyzed during the current study are not publicly
417 available but are available from the corresponding author on reasonable request.

418

419

420 **References:**

- 421 1. Funder JW, Carey RM, Mantero F, et al. The Management of Primary Aldosteronism:
422 Case Detection, Diagnosis, and Treatment: An Endocrine Society Clinical Practice
423 Guideline. *J Clin Endocrinol Metab.* 2016;**101**(5):1889-1916
- 424 2. Monticone S, Burrello J, Tizzani D, et al. Prevalence and Clinical Manifestations of
425 Primary Aldosteronism Encountered in Primary Care Practice. *J Am Coll Cardiol.*
426 2017;**69**(14):1811-1820
- 427 3. Hannemann A, Wallaschofski H. Prevalence of primary aldosteronism in patient's
428 cohorts and in population-based studies--a review of the current literature. *Horm Metab*
429 *Res.* 2012;**44**(3):157-162
- 430 4. Brown JM, Siddiqui M, Calhoun DA, et al. The Unrecognized Prevalence of Primary
431 Aldosteronism. *Ann Intern Med.* 2020; **173**(1):10-20
- 432 5. Savard S, Amar L, Plouin PF, Steichen O. Cardiovascular complications associated with
433 primary aldosteronism: a controlled cross-sectional study. *Hypertension.*
434 2013;**62**(2):331-336
- 435 6. Monticone S, D'Ascenzo F, Moretti C, et al. Cardiovascular events and target organ
436 damage in primary aldosteronism compared with essential hypertension: a systematic
437 review and meta-analysis. *Lancet Diabetes Endocrinol.* 2018;**6**(1):41-50
- 438 7. Fernandes-Rosa FL, Boulkroun S, Zennaro MC. Genetic and Genomic Mechanisms of
439 Primary Aldosteronism. *Trends Mol Med.* 2020;**26**(9):819-832
- 440 8. Nanba K, Omata K, Else T, et al. Targeted Molecular Characterization of Aldosterone-
441 Producing Adenomas in White Americans. *J Clin Endocrinol Metab.*
442 2018;**103**(10):3869-3876
- 443 9. Nanba K, Omata K, Gomez-Sanchez CE, et al. Genetic Characteristics of Aldosterone-
444 Producing Adenomas in Blacks. *Hypertension.* 2019;**73**(4):885-892
- 445 10. De Sousa K, Boulkroun S, Baron S, et al. Genetic, Cellular, and Molecular
446 Heterogeneity in Adrenals With Aldosterone-Producing Adenoma. *Hypertension.*
447 2020;**75**(4):1034-1044
- 448 11. Ono Y, Yamazaki Y, Omata K, et al. Histological Characterization of Aldosterone-
449 producing Adrenocortical Adenomas with Different Somatic Mutations. *J Clin*
450 *Endocrinol Metab.* 2020;**105**(3):e282-e289
- 451 12. Nanba K, Yamazaki Y, Bick N, et al. Prevalence of Somatic Mutations in Aldosterone-
452 Producing Adenomas in Japanese Patients. *J Clin Endocrinol Metab.* 2020;**105**(11):
453 e4066-e4073
- 454 13. Williams TA, Gomez-Sanchez CE, Rainey WE, et al. International Histopathology
455 Consensus for Unilateral Primary Aldosteronism. *J Clin Endocrinol Metab.*
456 2021;**106**(1):42-54
- 457 14. Nishimoto K, Tomlins SA, Kuick R, et al. Aldosterone-stimulating somatic gene
458 mutations are common in normal adrenal glands. *Proc Natl Acad Sci U S A.*
459 2015;**112**(33):E4591-4599
- 460 15. Nishimoto K, Seki T, Kurihara I, et al. Case Report: Nodule Development From
461 Subcapsular Aldosterone-Producing Cell Clusters Causes Hyperaldosteronism. *J Clin*
462 *Endocrinol Metab.* 2016;**101**(1):6-9
- 463 16. Scholl UI, Healy JM, Thiel A, et al. Novel somatic mutations in primary
464 hyperaldosteronism are related to the clinical, radiological and pathological phenotype.
465 *Clin Endocrinol (Oxf).* 2015;**83**(6):779-789
- 466 17. Akerstrom T, Maharjan R, Sven Willenberg H, et al. Activating mutations in CTNNB1
467 in aldosterone producing adenomas. *Sci Rep.* 2016;**6**:19546

- 468 **18.** Zhou J, Azizan EAB, Cabrera CP, et al. Somatic mutations of GNA11 and GNAQ in
469 CTNNB1-mutant aldosterone-producing adenomas presenting in puberty, pregnancy or
470 menopause. [published ahead of print August 12, 2021]. *Nat Genet.* doi:
471 [10.1038/s41588-021-00906-y](https://doi.org/10.1038/s41588-021-00906-y)
- 472 **19.** Rhayem Y, Perez-Rivas LG, Dietz A, et al. PRKACA Somatic Mutations Are Rare
473 Findings in Aldosterone-Producing Adenomas. *J Clin Endocrinol Metab.*
474 2016;**101**(8):3010-3017
- 475 **20.** Drelon C, Berthon A, Mathieu M, Martinez A, Val P. Adrenal cortex tissue homeostasis
476 and zonation: A WNT perspective. *Mol Cell Endocrinol.* 2015;**408**:156-164
- 477 **21.** Pignatti E, Leng S, Yuchi Y, et al. Beta-Catenin Causes Adrenal Hyperplasia by
478 Blocking Zonal Transdifferentiation. *Cell Rep.* 2020;**31**(3):107524
- 479 **22.** Connell JM, Davies E. The new biology of aldosterone. *J Endocrinol.* 2005;**186**(1):1-
480 20
- 481 **23.** Hattangady NG, Olala LO, Bollag WB, Rainey WE. Acute and chronic regulation of
482 aldosterone production. *Mol Cell Endocrinol.* 2012;**350**(2):151-162
- 483 **24.** Duparc C, Moreau L, Dzib JF, et al. Mast cell hyperplasia is associated with aldosterone
484 hypersecretion in a subset of aldosterone-producing adenomas. *J Clin Endocrinol*
485 *Metab.* 2015;**100**(4):E550-560
- 486 **25.** Ehrhart-Bornstein M, Hinson JP, Bornstein SR, Scherbaum WA, Vinson GP.
487 Intraadrenal interactions in the regulation of adrenocortical steroidogenesis. *Endocr*
488 *Rev.* 1998;**19**(2):101-143
- 489 **26.** Wils J, Duparc C, Cailleux AF, et al. The neuropeptide substance P regulates
490 aldosterone secretion in human adrenals. *Nat Commun.* 2020;**11**(1):2673
- 491 **27.** Lopez AG, Duparc C, Naccache A, et al. Role of Mast Cells in the Control of
492 Aldosterone Secretion. *Horm Metab Res.* 2020;**52**(6):412-420
- 493 **28.** Theoharides TC. Neuroendocrinology of mast cells: Challenges and controversies. *Exp*
494 *Dermatol.* 2017;**26**(9):751-759
- 495 **29.** Hinson JP, Vinson GP, Kapas S, Teja R. The relationship between adrenal vascular
496 events and steroid secretion: the role of mast cells and endothelin. *J Steroid Biochem*
497 *Mol Biol.* 1991;**40**(1-3):381-389
- 498 **30.** Thomas M, Keramidas M, Monchaux E, Feige JJ. Role of adrenocorticotrophic hormone
499 in the development and maintenance of the adrenal cortical vasculature. *Microsc Res*
500 *Tech.* 2003;**61**(3):247-251
- 501 **31.** Feige JJ. Angiogenesis in adrenocortical physiology and tumor development. *Ann*
502 *Endocrinol (Paris).* 2009;**70**(3):153-155
- 503 **32.** Funder JW, Carey RM, Fardella C, et al. Case detection, diagnosis, and treatment of
504 patients with primary aldosteronism: an endocrine society clinical practice guideline. *J*
505 *Clin Endocrinol Metab.* 2008;**93**(9):3266-3281
- 506 **33.** Amar L, Baguet JP, Bardet S, et al. SFE/SFHTA/AFCE primary aldosteronism
507 consensus: Introduction and handbook. *Ann Endocrinol (Paris).* 2016;**77**(3):179-186
- 508 **34.** Baron S, Amar L, Faucon AL, et al. Criteria for diagnosing primary aldosteronism on
509 the basis of liquid chromatography-tandem mass spectrometry determinations of plasma
510 aldosterone concentration. *J Hypertens.* 2018;**36**(7):1592-1601
- 511 **35.** Webb TR, Clark AJ. Minireview: the melanocortin 2 receptor accessory proteins. *Mol*
512 *Endocrinol.* 2010;**24**(3):475-484
- 513 **36.** Pignatti E, Leng S, Carlone DL, Breault DT. Regulation of zonation and homeostasis in
514 the adrenal cortex. *Mol Cell Endocrinol.* 2017;**441**:146-155
- 515 **37.** Lefebvre H, Compagnon P, Contesse V, et al. Production and metabolism of serotonin
516 (5-HT) by the human adrenal cortex: paracrine stimulation of aldosterone secretion by
517 5-HT. *J Clin Endocrinol Metab.* 2001;**86**(10):5001-5007

- 518 **38.** Boyer HG, Wils J, Renouf S, et al. Dysregulation of Aldosterone Secretion in Mast Cell-
519 Deficient Mice. *Hypertension*. 2017;**70**(6):1256-1263
- 520 **39.** Hinson JP, Vinson GP, Pudney J, Whitehouse BJ. Adrenal mast cells modulate vascular
521 and secretory responses in the intact adrenal gland of the rat. *J Endocrinol*.
522 1989;**121**(2):253-260
- 523 **40.** Berthon A, Drelon C, Ragazzon B, et al. WNT/beta-catenin signalling is activated in
524 aldosterone-producing adenomas and controls aldosterone production. *Hum Mol Genet*.
525 2014;**23**(4):889-905
- 526 **41.** Vouillarmet J, Fernandes-Rosa F, Graeppi-Dulac J, et al. Aldosterone-Producing
527 Adenoma With a Somatic KCNJ5 Mutation Revealing APC-Dependent Familial
528 Adenomatous Polyposis. *J Clin Endocrinol Metab*. 2016;**101**(11):3874-3878
- 529 **42.** Ye P, Mariniello B, Mantero F, Shibata H, Rainey WE. G-protein-coupled receptors in
530 aldosterone-producing adenomas: a potential cause of hyperaldosteronism. *J*
531 *Endocrinol*. 2007;**195**(1):39-48
- 532 **43.** Novoselova TV, Jackson D, Campbell DC, Clark AJ, Chan LF. Melanocortin receptor
533 accessory proteins in adrenal gland physiology and beyond. *J Endocrinol*.
534 2013;**217**(1):R1-11
- 535 **44.** El Ghorayeb N, Bourdeau I, Lacroix A. Role of ACTH and Other Hormones in the
536 Regulation of Aldosterone Production in Primary Aldosteronism. *Front Endocrinol*
537 *(Lausanne)*. 2016;**7**:72
- 538 **45.** Gallo-Payet N. 60 YEARS OF POMC: Adrenal and extra-adrenal functions of ACTH.
539 *J Mol Endocrinol*. 2016;**56**(4):T135-156
- 540 **46.** Soucek L, Lawlor ER, Soto D, et al. Mast cells are required for angiogenesis and
541 macroscopic expansion of Myc-induced pancreatic islet tumors. *Nat Med*.
542 2007;**13**(10):1211-1218
- 543 **47.** Lefebvre H, Thomas M, Duparc C, Bertherat J, Louiset E. Role of ACTH in the
544 Interactive/Paracrine Regulation of Adrenal Steroid Secretion in Physiological and
545 Pathophysiological Conditions. *Front Endocrinol (Lausanne)*. 2016;**7**:98
- 546 **48.** Sasano H, Suzuki T, Moriya T. Adrenal Cortex. In: Lloyd RV (eds). *Endocrine*
547 *Pathology*. Humana Press: Totowa; 2004.
- 548 **49.** Boulkroun S, Samson-Couterie B, Golib-Dzib JF, et al. Aldosterone-producing
549 adenoma formation in the adrenal cortex involves expression of stem/progenitor cell
550 markers. *Endocrinology*. 2011;**152**(12):4753-4763
- 551 **50.** Louiset E, Duparc C, Lefebvre H. Role of serotonin in the paracrine control of adrenal
552 steroidogenesis in physiological and pathophysiological conditions. *Current Opinion in*
553 *Endocrine and Metabolic Research*. 2019;**8**:50-59
- 554 **51.** Lefebvre H, Duparc C, Naccache A, et al. Paracrine Regulation of Aldosterone
555 Secretion in Physiological and Pathophysiological Conditions. *Vitam Horm*.
556 2019;**109**:303-339

557

558

Table 1. Samples analyzed in this study.

Patient ID	Structure	CYP11B2 staining	Mutation	Multiplex Immunofluorescence study	Gene expression study
1	APA	Yes	<i>ATP2B3</i>	Yes	
4	APA	Yes	<i>CACNA1D</i>	Yes	
	APCC3	Yes	<i>CACNA1D</i>	Yes	
	APCC4	Yes	<i>KCNJ5</i>	Yes	
	APCC5	Yes	<i>Neg</i>	Yes	
	APCC6	Yes	<i>Neg</i>	Yes	
	APCC7	Yes	<i>Neg</i>	Yes	
8	APA	Yes	<i>CACNA1D</i>	Yes	
10	APA	Yes	<i>CACNA1D</i>		Yes
24	APA	Yes	<i>ATP1A1</i>	Yes	
25	APA	Yes	<i>Neg</i>		Yes
26	APA	Yes	<i>ATP1A1</i>	Yes	
34	APA	Yes	<i>CACNA1D</i>		Yes
36	APA	Yes	<i>ATP2B3</i>	Yes	
40	APA	Yes	<i>KCNJ5</i>		
	APA zone 1	No	<i>KCNJ5</i>		Yes
	APA zone 2	Yes	<i>KCNJ5</i>		Yes
	APA zone 3	Yes	<i>KCNJ5</i>		Yes
	APA zone 4	No	<i>KCNJ5</i>		Yes
41	APA	Yes	<i>CACNA1D</i>	Yes	
	APCC1	Yes	<i>Neg</i>	Yes	
	APCC2	Yes	<i>CACNA1D</i>	Yes	
	APCC4	Yes	<i>CACNA1D</i>	Yes	
			<i>CACNA1D</i>	Yes	
			<i>CACNA1H</i>	Yes	
	APCC5	Yes	<i>KCNJ5</i>	Yes	
42	APA	Yes	<i>CACNA1D</i>		Yes
50	APA	Yes	<i>KCNJ5</i>	Yes	
	APA zone 1	No	<i>KCNJ5</i>		Yes
	APA zone 2	Yes	<i>KCNJ5</i>		Yes
52	APA	Yes	<i>KCNJ5</i>	Yes	
	APCC2	Yes	<i>CACNA1D</i>	Yes	
	APCC4	Yes	<i>KCNJ5</i>	Yes	
	APCC1	Yes	<i>Neg</i>	Yes	
	APCC3	Yes	<i>Neg</i>	Yes	
53	APA	Yes	<i>ATP1A1</i>	Yes	
56	APA	Yes	<i>ATP2B3</i>	Yes	Yes
	Nodule	No	<i>Neg</i>	Yes	Yes
48 bloc1	APCC1	Yes	<i>CACNA1D</i>	Yes	
	APCC2	Yes	<i>Neg</i>	Yes	
	APCC3	Yes	<i>CACNA1D</i>	Yes	
	APCC6	Yes	<i>CACNA1D</i>	Yes	
48 bloc4	pAATL B2+	Yes	<i>CACNA1D</i>	Yes	
	pAATL B2-	No	<i>CACNA1D</i>	Yes	

561 **Figure legends**

562

563 **Figure 1. Signaling pathways and cellular environment in APA.** A, Colocalization of
564 CYP11B2 (aldosterone-synthase), CYP17A1 (17 α -hydroxylase), β -catenin, MC2R
565 (melanocortin receptor type 2) and pCREB by multiplex immunofluorescence in APA. B.
566 Colocalization of CYP11B2, CD34 (vessels), Tryptase (mast cells), S100 (nerve fibers) by
567 multiplex immunofluorescence in APA. Images represent the APA from patient 1 carrying an
568 *ATP2B3* mutation.

569

570 **Figure 2. Distribution of components of the microenvironment in different regions of**
571 **APA.** The number of mast cells (stained by Tryptase $p < 0.0001$ (A-B)), the vessels surface
572 (stained by CD34, $p = 0.1214$) (C), and the number of nerve fibers (stained by S100 $p = 0.7346$)
573 (D) were quantified in APA regions expressing aldosterone synthase (CYP11B2+) or not
574 expressing aldosterone synthase (CYP11B2-) using InForm. 11 APAs carrying *ATP1A1* (n=3),
575 *ATP2B3* (n=2), *CACNA1D* (n=3), and *KCNJ5* (n=2) mutations were analyzed. P-values were
576 calculated only for the entire set of APA (all, n=11).

577

578 **Figure 3. Interaction between nerve fibers and mast cells in APA.** A. The distance between
579 mast cells (stained by tryptase, green) and nerve fibers (stained by S100, cyan) was measured
580 in 11 APAs carrying *ATP1A1* (n=3), *ATP2B3* (n=2), *CACNA1D* (n=3), and *KCNJ5* (n=2)
581 mutations. B. Quantification of the distances between mast cells and nerve fibers as analysed
582 in (A) represented as the mean of all measures for each individual APA (All) or individually
583 for each APA. CYP11B2 (yellow), DAPI (nuclei, blue); white arrows indicate nerve fibers.

584 **Figure 4. Perivascular localization of mast cells in APA.** APA tissues from three patients
585 carrying different mutations were stained by multiplex immunofluorescence for localisation of
586 mast cells (Tryptase - green) and vessels (CD34 - Magenta). ADJ: adjacent adrenal cortex.
587 Nuclei are stained in blue by DAPI.

588

589 **Figure 5. Expression of components of PKA signaling in APA.** Automatic quantification of
590 colocalization of different proteins was analysed in the entire set of 11 APAs and by mutation
591 status (*ATP1A1*, n=3; *ATP2B3*, n=3; *CACNA1D*, n=3; *KCNJ5*, n=2). Colocalization of
592 CYP11B2-MC2R (A), CYP17A1-MC2R (B), CYP11B2-pCREB (C), CYP17A1-pCREB (D)
593 and MC2R-pCREB (E). White bars refer to the percentage of cells expressing only the first
594 marker: CYP11B2 (A and C), CYP17A1 (B and D), and MC2R (E). Grey bars refer to the
595 percentage of cells co-expressing the second marker together with the first. P-values were
596 calculated only for the entire set of APA (all, n=11). ****, p<0.0001; ***, p<0.001.

597

598 **Figure 6. Expression of genes involved in ACTH/cAMP signalling and vascularization.** (A)
599 Aldosterone synthase (CYP11B2) and (B) 11 β hydroxylase (CYP11B1) staining in APA from
600 5 patients. RNA was extracted from five APA (patients 25, 34, 42, 10, and 56) and from one
601 nodule not expressing CYP11B2 from patient 56. mRNA expression of MC2R (C), MRAP (D))
602 and VEGFA (E) was assessed by RT-qPCR. Relative mRNA expression represents mRNA
603 levels of the gene of interest normalized by the geometric mean of two housekeeping genes.

604

605 **Figure 7. Expression of genes involved in ACTH/cAMP signaling and vascularization and**
606 **intratumoral heterogeneity in *KCNJ5* mutated APA.** (A) Areas with different aldosterone
607 synthase expression from 2 APA carrying a *KCNJ5* mutation (according to (10)) were

608 investigated. RNA was extracted from one CYP11B2-positive region and one region with
609 mostly negative expression of CYP11B2 from patient 50, two CYP11B2-positive regions and
610 two regions with mostly negative expression of CYP11B2 from patient 40. mRNA expression
611 of *MC2R* (B), *MRAP* (C) and *VEGFA* (D) was assessed by RT-qPCR. Relative mRNA
612 expression represents mRNA levels of the gene of interest normalized by the geometric mean
613 of two housekeeping genes.

614

615 **Figure 8. Expression and activation of signaling pathways and paracrine pathways in**
616 **APCC.** Colocalization of CD34 (vessels), S100 (nerve fibers), Tryptase (mast cells), CYP11B2
617 (aldosterone-synthase), CYP17A1 (17 α -hydroxylase), β -catenin and pCREB by multiplex
618 immunofluorescence in one APCC from an adrenal with multinodular hyperplasia (A) and in
619 one APCC from an adrenal with APA (B).

620

621 **Figure 9. Comparison between IHC and multiplex immunofluorescence in APCC.** For
622 technical reasons, acquisition of MC2R marking on opal was not possible, thus we have
623 investigated in IHC expression of all other markers in the same APCCs analyzed in multiplex
624 immunofluorescence.

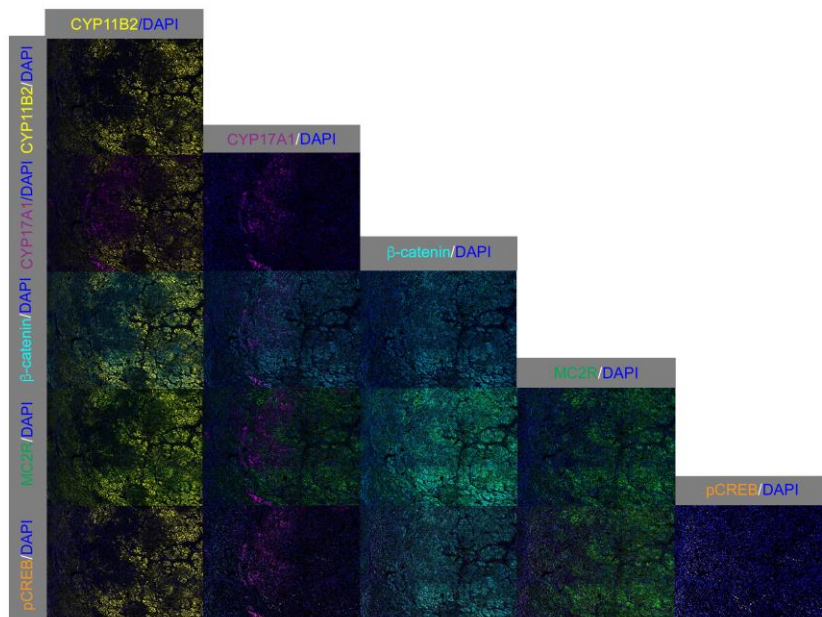
625

626 **Figure 10: Expression and activation of signalling pathways and paracrine pathways in**
627 **pAATL.** (A) HES and (B) CYP11B2 staining in one adrenal (patient 48) with micronodular
628 hyperplasia showing the presence of one pAATL. (C) Expression of CD34 (vessels), S100
629 (nerve fibers), Tryptase (mast cells), CYP11B2 (aldosterone-synthase), CYP17A1 (17 α -
630 hydroxylase), β -catenin, MC2R (melanocortin receptor type 2), and pCREB by multiplex
631 immunofluorescence.

632

633 **Figure 11: Wnt/ β -catenin and ACTH/cAMP signaling in a nodule not expressing**
634 **aldosterone synthase in an adrenal with APA.** Colocalization of CYP11B2 (aldosterone
635 synthase), CYP17A1 (17 α -hydroxylase), β -catenin, MC2R (melanocortin receptor type 2) and
636 pCREB by multiplex immunofluorescence in a nodule not expressing aldosterone synthase in
637 one adrenal with APA (patient 56).

A



B

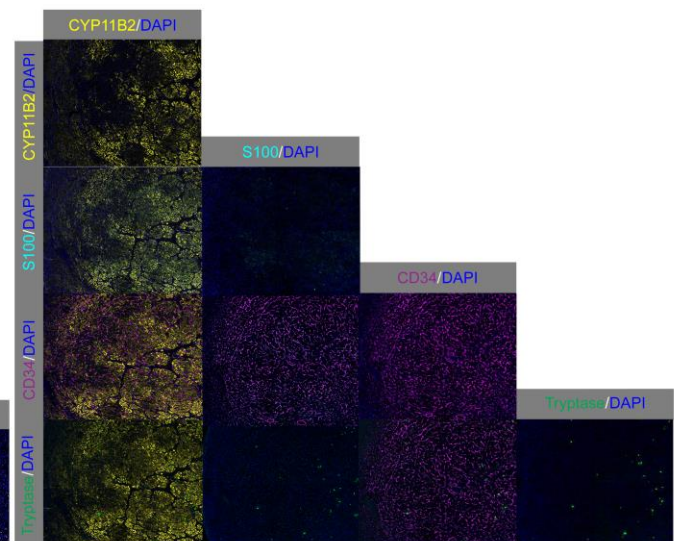


Figure 1

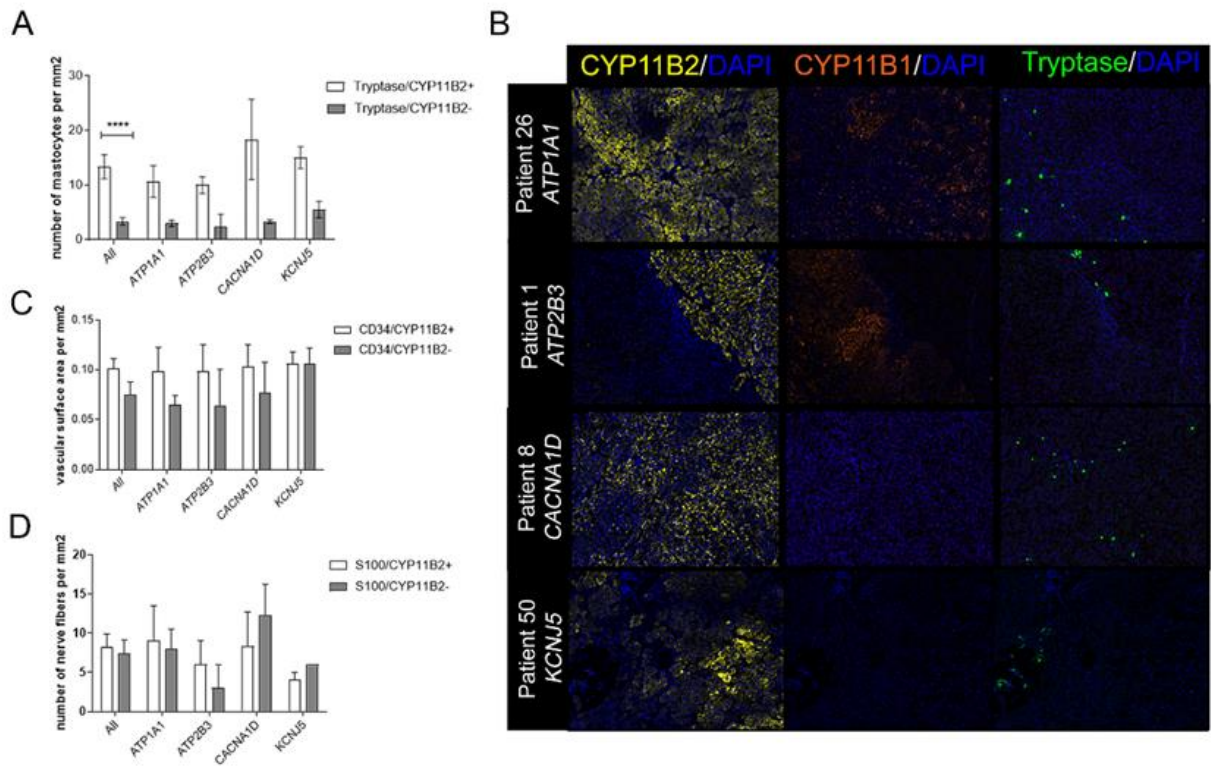


Figure 2

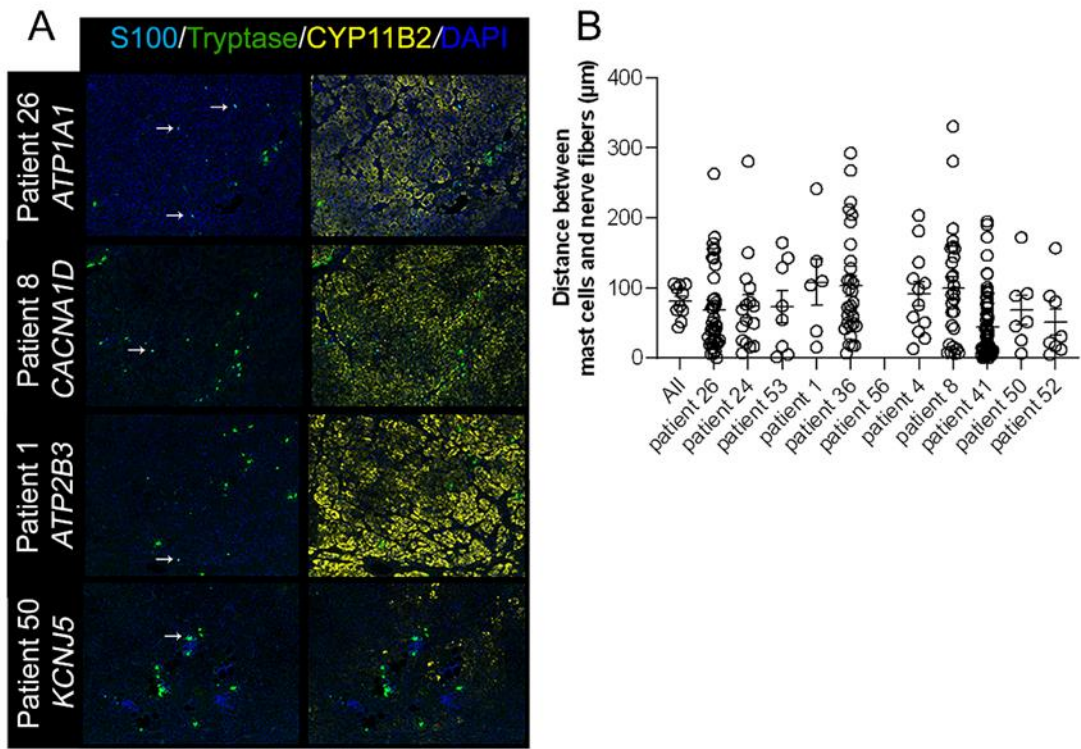


Figure 3

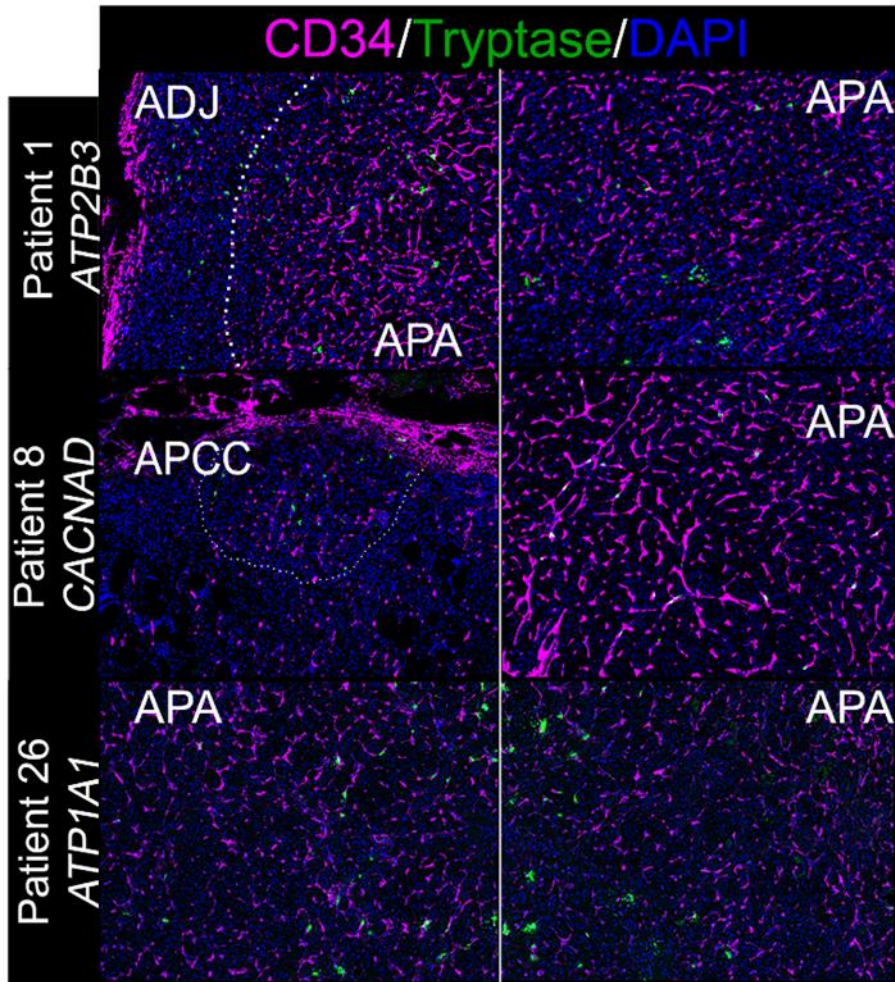


Figure 4

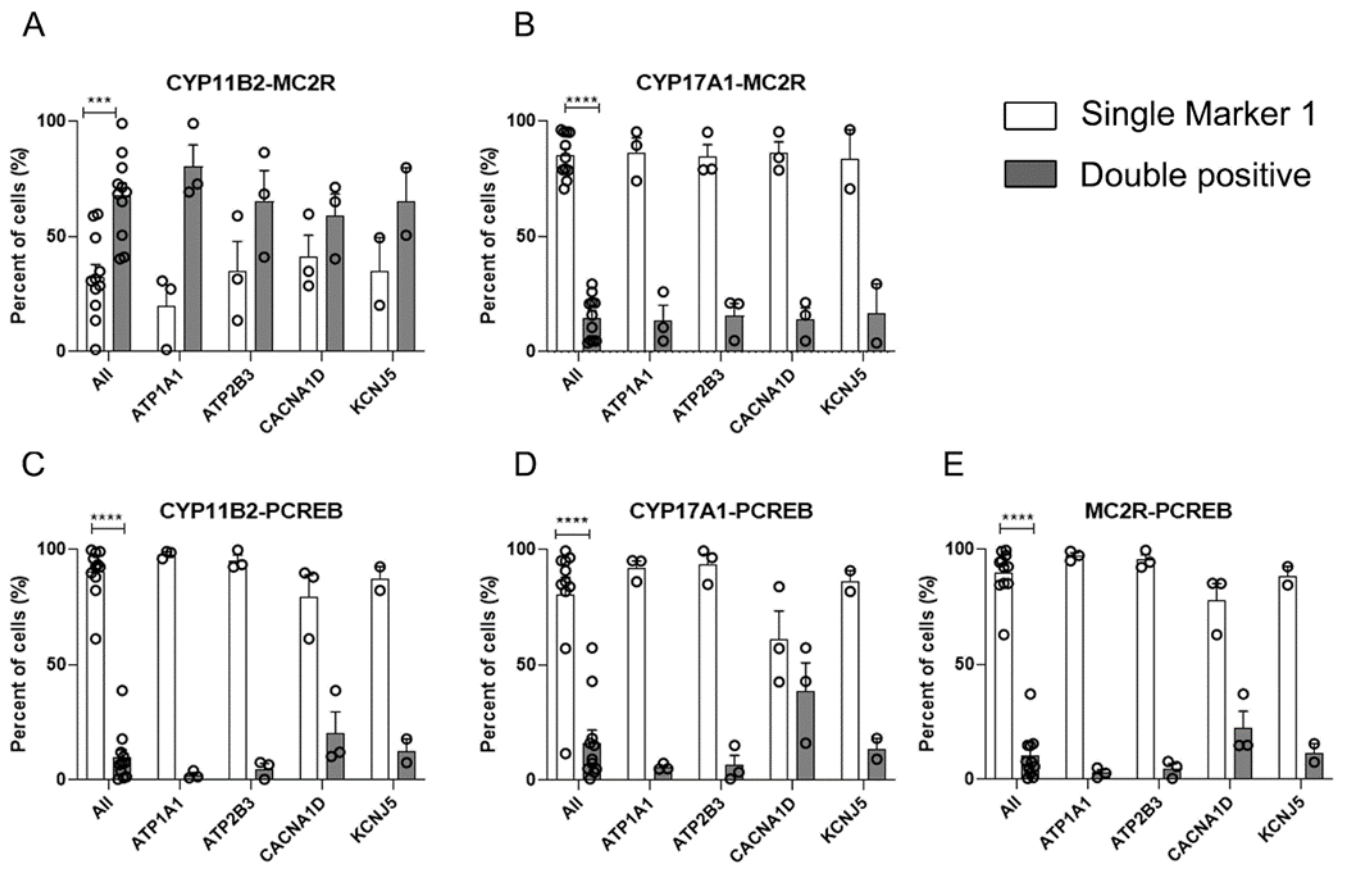


Figure 5

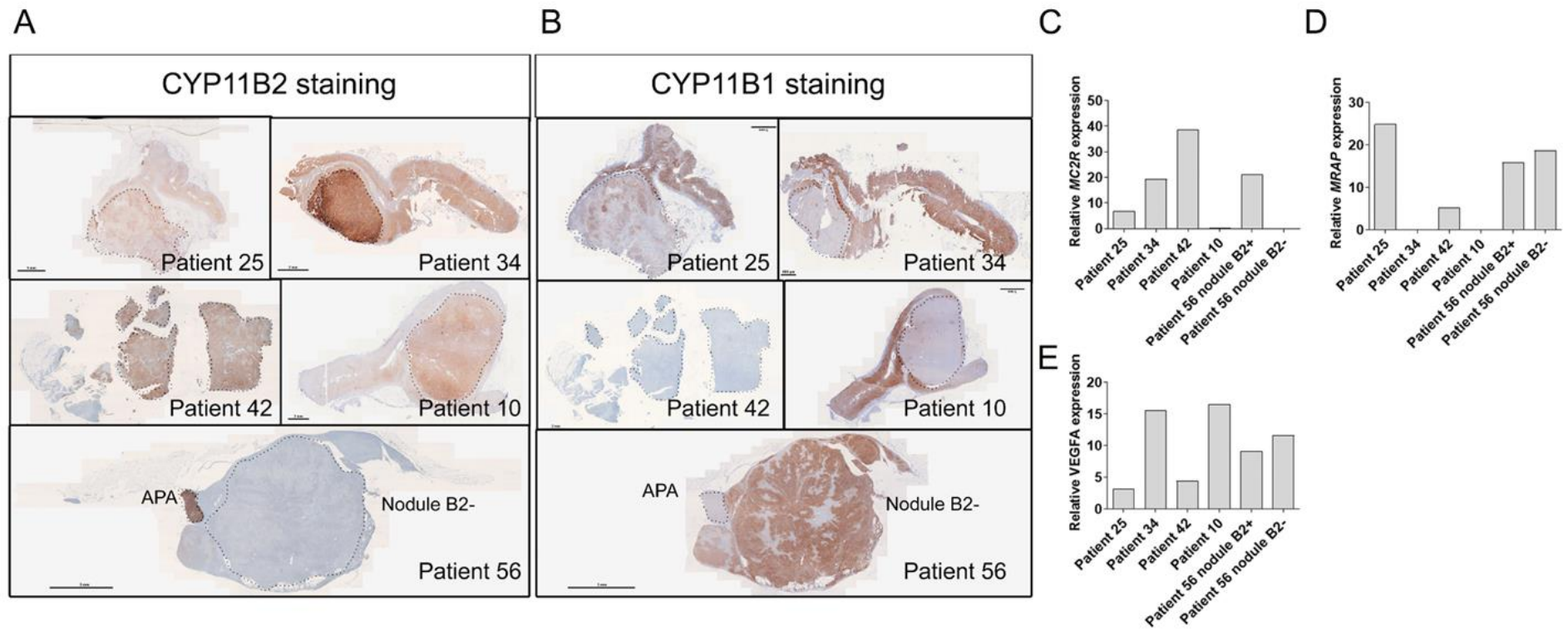
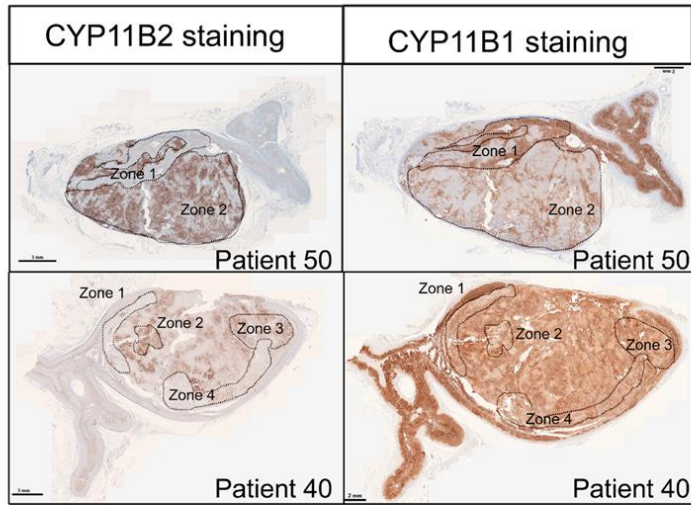
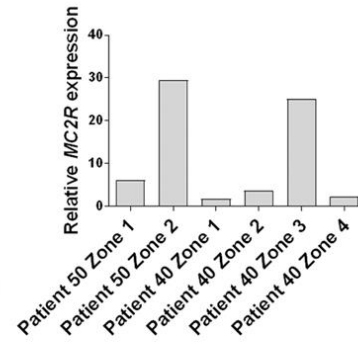


Figure 6

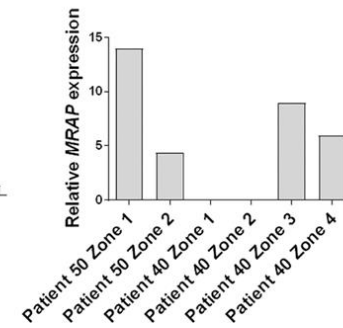
A



B



C



D

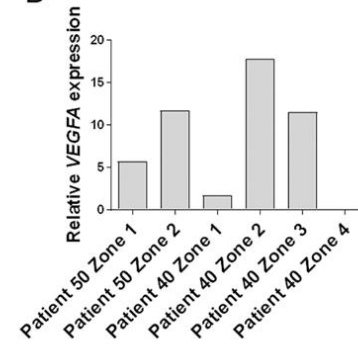


Figure 7

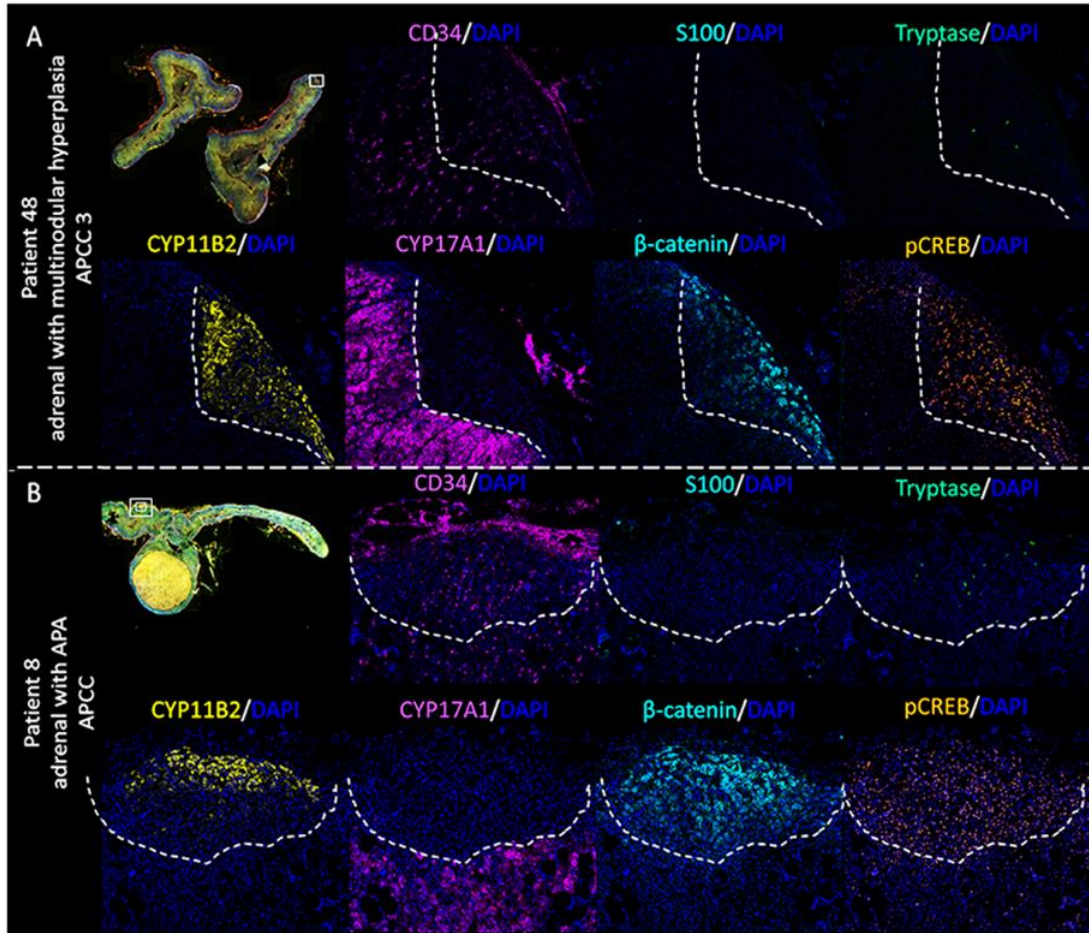


Figure 8

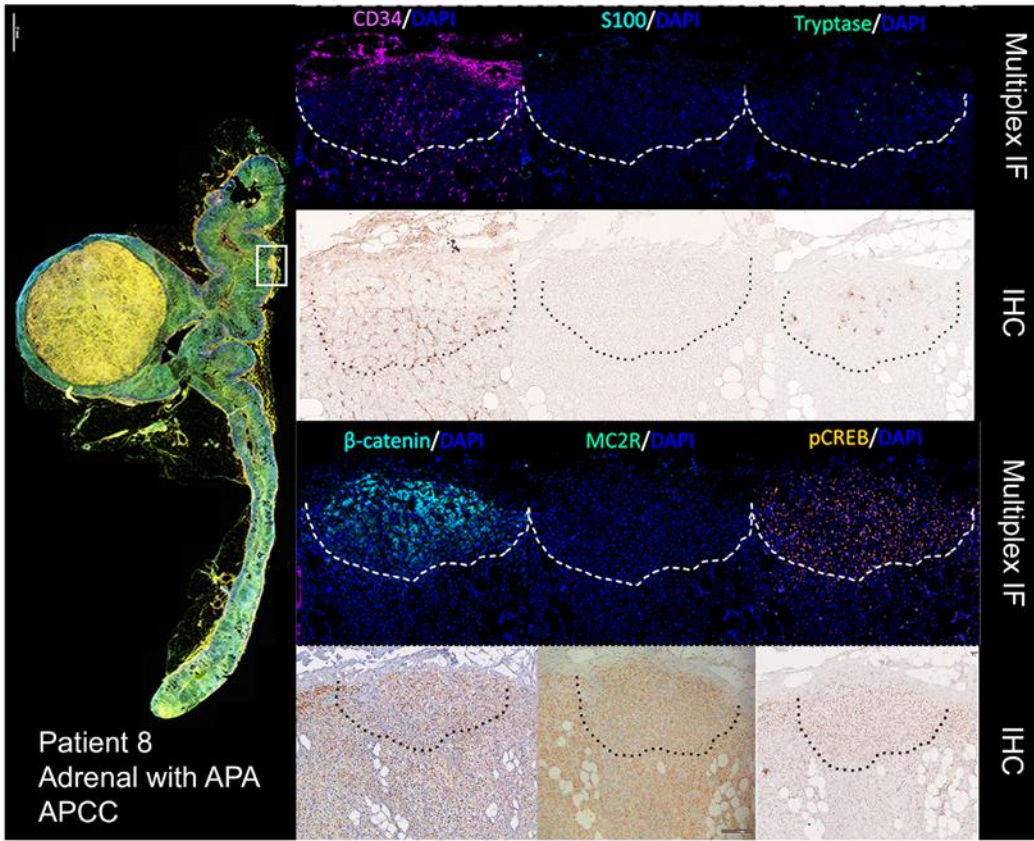


Figure 9

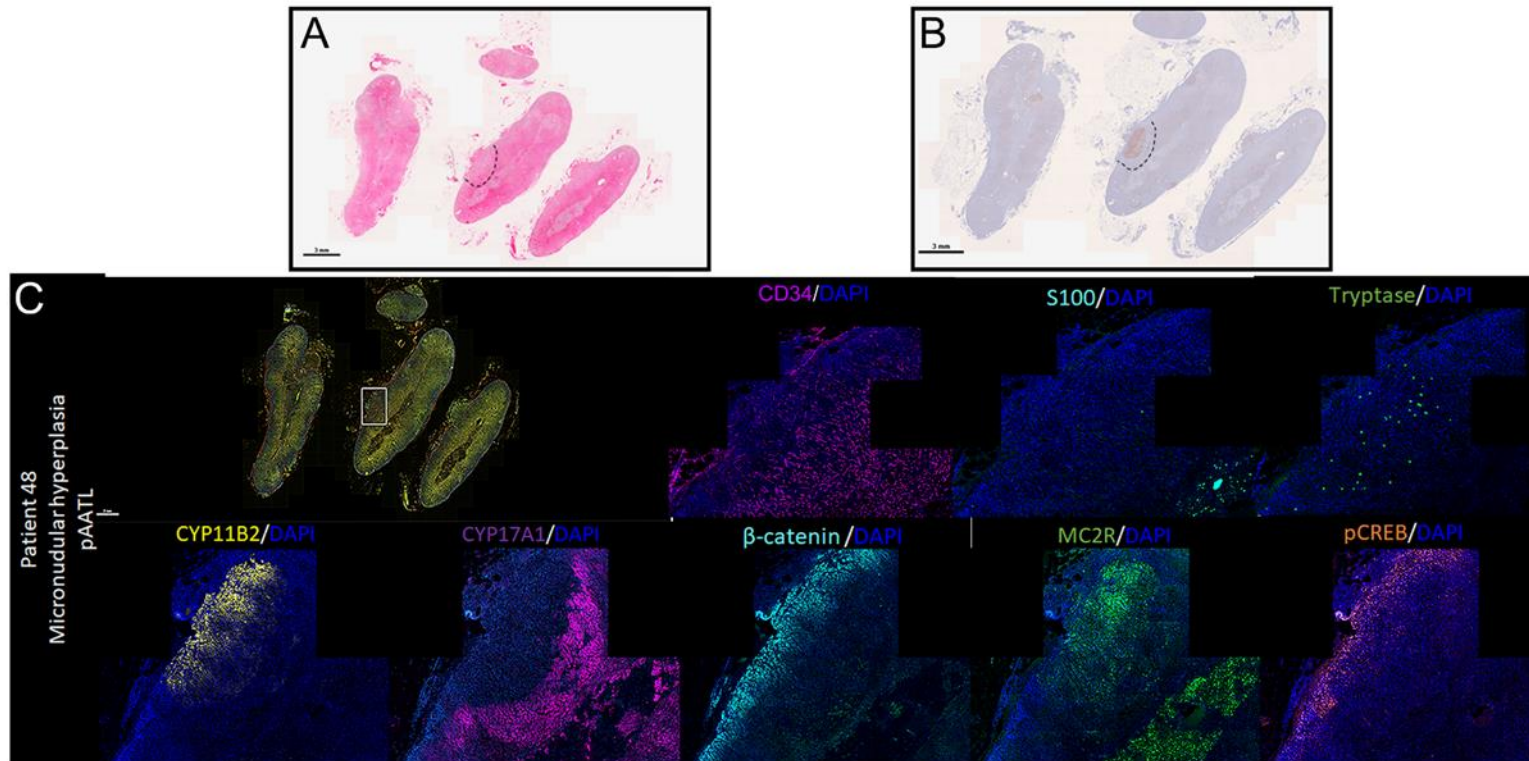


Figure 10

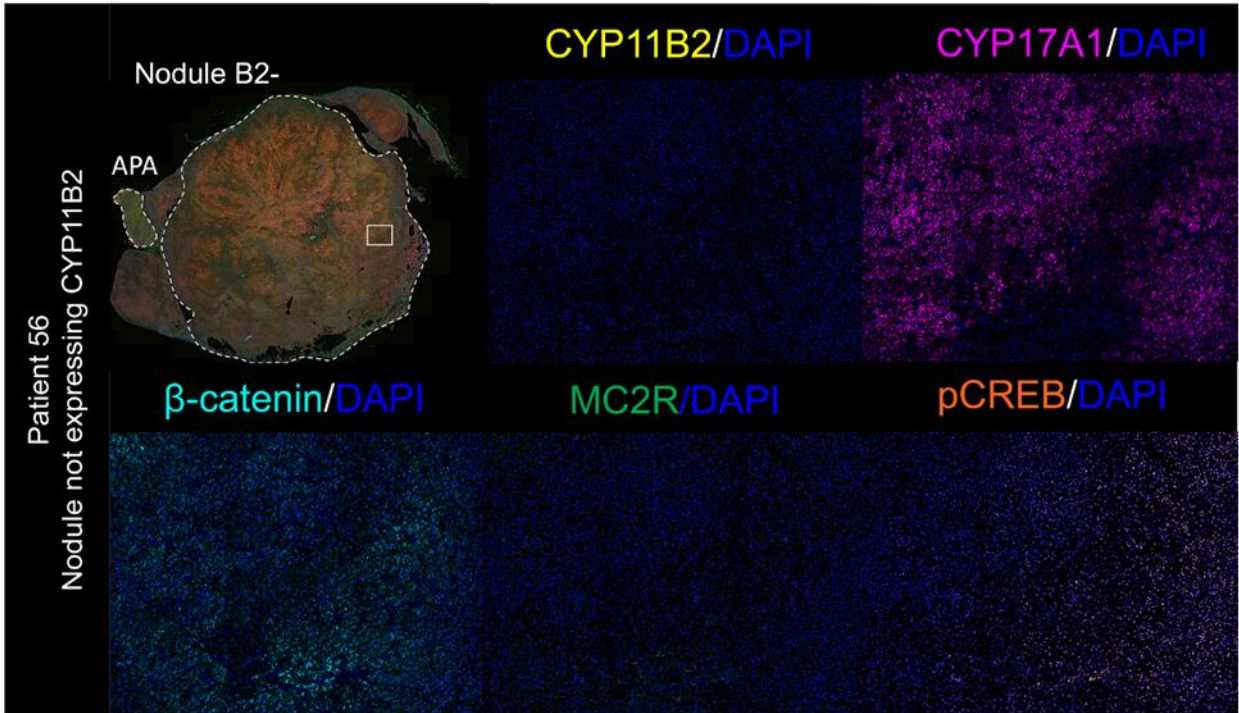


Figure 11